

# Reservoir Characterization to Optimize CO<sub>2</sub> Injection

A. Gordon<sup>1</sup>, E. Mutual<sup>1\*</sup>, R. Cova<sup>1</sup>, B. Goodway<sup>1</sup>, W. Pardasie<sup>1</sup>, M. Ng<sup>2</sup>, S. Tracey<sup>3</sup> Advantage Energy

<sup>1</sup>Qeye, Calgary, Alberta, Canada

<sup>2</sup>Entropy Inc., Calgary, Alberta, Canada

<sup>3</sup>Advantage Energy Ltd., Calgary, Alberta, Canada

## Abstract

Carbon capture, utilization, and storage (CCUS) projects require detailed reservoir characterization to ensure safe and effective CO<sub>2</sub> injection. This study focuses on the Triassic Baldonnel Formation in western Canada as a target for CO<sub>2</sub> sequestration. We applied a deterministic Amplitude-Versus-Offset (AVO) seismic inversion using a three-term Aki–Richards linear approximation (Aki and Richards, 1980) to obtain elastic properties in the Baldonnel. Comprehensive seismic data conditioning (including azimuthal alignment, amplitude balancing, and bandpass filtering) was performed to improve inversion fidelity. A robust low-frequency model (LFM) was built by integrating one key well log with seismic processing velocities, adjusted via time shifts obtained from the alignment. Then, a rock physics inversion was conducted using a regression-based model constrained by theoretical bounds (Voigt, Reuss, and Hashin–Shtrikman limits) and multi-mineral fluid substitution using Gassmann’s equation. The rock physics model was calibrated explicitly for the Baldonnel formation’s mixed lithology consisting primarily of dolomite and limestone with clay and siltstone interbeds. The inversion predicts spatial distributions of porosity and mineral fractions (clay, calcite, dolomite) across the reservoir, which serve as critical inputs for reservoir modeling and simulation.

Results reveal that higher porosity zones in the Baldonnel are laterally continuous where dolomitization is prevalent, whereas deeper intervals lack significant porosity. A horizontal CO<sub>2</sub> injector well drilled post-inversion confirmed the absence of high porosities in the lower Baldonnel, validating the inversion’s predictions. The operator is currently injecting ~40 tonnes of CO<sub>2</sub> per day into the Baldonnel and plans to scale up to ~500 tonnes/day in the near future. Our study provides valuable insights into using deterministic seismic inversion for CCUS: by integrating rock physics and inversion products into dynamic models, we optimize injectivity and storage capacity while ensuring containment. New porosity maps based on this workflow demonstrate significantly improved reservoir characterization when seismic inversion is incorporated, compared to maps derived only from available well control. These outcomes underline the impact of advanced geophysical workflows on CO<sub>2</sub> injection planning and set a precedent for CCUS best practices in similar reservoirs.

## Introduction

Climate change mitigation efforts have intensified interest in geological CO<sub>2</sub> sequestration, requiring subsurface reservoirs that can safely accept and store large volumes of CO<sub>2</sub>. The Triassic Baldonnel Formation, a carbonate unit in the Western Canadian Sedimentary Basin, is being evaluated as a CO<sub>2</sub> injection target in northwest Alberta. The Baldonnel is a known dolomitic carbonate with interbedded clastics; in many areas it exhibits excellent reservoir quality with porosities up to 30%, although freshwater flushing has precipitated bitumen and reduced pore space in places. Selecting and qualifying such a formation for CO<sub>2</sub> storage demands thorough reservoir characterization to ensure sufficient porosity, permeability, and caprock integrity (IPCC, 2005). Traditional site selection criteria for CO<sub>2</sub> storage emphasize reservoirs with adequate thickness and high porosity, along with reliable seals (Bachu, 2015). In this study, we build upon these principles by applying an advanced quantitative interpretation workflow to the Baldonnel Formation, leveraging seismic AVO inversion and rock physics analysis to map spatial variability in reservoir properties critical to CO<sub>2</sub> injectivity and capacity.

This study is a continuation of a previous multi-formation study that demonstrated the value of integrating seismic inversion with rock physics for simultaneous gas production and CO<sub>2</sub> storage (Gordon et al., 2023). Where AVO inversion workflows were used to characterize four formations: Cadomin, Baldonnel, Montney and Belloy – by identifying the Montney as a hydrocarbon producer and the Cadomin/Baldonnel as CO<sub>2</sub> sequestration targets. The study showed that inverted elastic attributes combined with rock physics constraints can estimate porosity and mineralogy variations, improving understanding of caprock integrity and reservoir capacity. The present paper focuses exclusively on the Baldonnel Formation, expanding on that work to detail the methods and results pertinent to optimizing CO<sub>2</sub> injection in this carbonate reservoir.

## Methodology

The first step in our workflow was preparing or preconditioning the seismic data for AVO inversion. We had a 3D seismic survey covering the area of interest, with pre-stack time migrated (PSTM) gathers available. The data exhibited some anisotropy effects and minor processing misalignments that could jeopardize an AVO analysis if uncorrected. We therefore implemented the following data conditioning sequence.

The 3D seismic was acquired with a wide-azimuth geometry. Analysis of common-offset common-azimuth gathers showed slight azimuthal velocity variations. Therefore a seismic Velocity versus Azimuth (VVAZ) alignment was applied by deriving azimuth-dependent travel-time adjustments that flatten reflectors across all azimuth sectors. This step removed small timing inconsistencies and ensured that reflectors line up, thereby preserving true amplitude versus offset trends for subsequent inversion. The seismic alignment algorithm employs an iterative approach to optimize the cross-correlation coefficient of the energy envelope of adjacent angle stacks. A smoothly varying displacement field is calculated to align each angle stack to its adjacent stack and then summed to align each stack to the reference stack. The algorithm is amplitude preserving and is indifferent to the input amplitudes and phase, so polarity reversals from AVO signatures are accommodated and preserved. Then, the aligned azimuthal angle stacks are re-stacked into angle stacks ranging from 0-52°.

Amplitude inconsistencies observed as stripe-like bands across the seismic survey were addressed by applying a smooth constant correction to each angle-stack to balance the amplitudes ensuring that mid to far offsets were neither under- nor over-corrected relative to near offsets. A bandpass filter with a high-cut of 75 Hz was applied to remove high-frequency random noise beyond the seismic signal bandwidth. The aim was to preserve as much useful bandwidth as possible to increase inversion resolution.

Figure 1 show seismic sections of a near, mid and far angle-stack before and after the seismic precondition. It is noticeable how before preconditioning there is contamination from high frequency noise, mis-aligned events with respect to the interpreted horizons (mid and far) and amplitude discrepancies in stripe-like bands across the section. After the preconditioning, these effects are mitigated providing a cleaner and more suitable seismic section for the inversion.

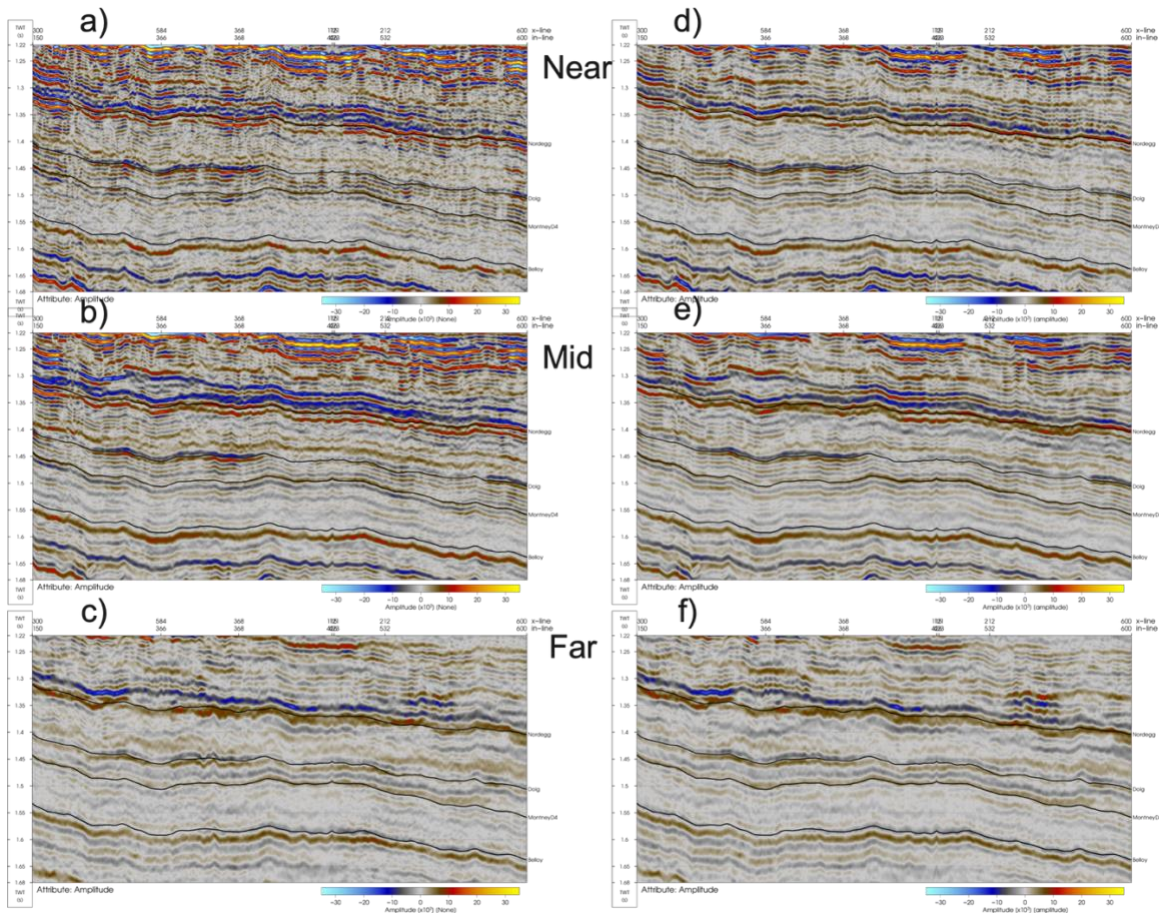


**Figure 1. Seismic section comparison of near, mid and far angle-stacks before and after seismic preconditioning. (a) near anglestack before condisioning, (b) mid anglestack before conditioning, (c) far anglestack before conditioning, (d) near anglestack after conditioning, (e) mid anglestack after conditioning, (c) far anglestack after conditioning. After the seismic conditioning, all these angle-stacks are less noisy, the reflection events are continuous across the section and follow the interpreted black horizons.**

The next key step for deterministic inversion is estimating angle-dependent wavelets from well log and seismic data. Angle reflectivity series are calculated from well logs and are tied to the seismic. Several estimation methods were tested including well log driven approaches versus seismic driven approaches like spectral and statistical methods. Ultimately a well log driven method yielded better results in the inversion test and was selected for the final inversion.

Using the conditioned angle-stacks and estimated angle-dependent wavelets, the workflow proceeded with the deterministic AVO inversion. We utilized a simultaneous inversion algorithm that inverts all angle stacks jointly for three elastic parameters (acoustic impedance (AI),  $V_p$ - $V_s$  ratio, and density). The forward model is the Aki-Richards equation (3-term) linearized reflection coefficient approximation (Aki and Richards, 1980). This equation relates the reflection amplitude at incidence angle to changes in P and S impedance and density. Angle stacks ranging from 5 to 45 degrees were inverted simultaneously by minimizing the misfit between observed and modeled reflectivity.

A low-frequency model (LFM) provided the initial models and trends for AI,  $V_p$ - $V_s$  ratio and density. To build a less biased LFM, a single well was used with the interpreted horizons and updated seismic processing velocities to incorporate more realistic spatial variability into the model. The simultaneous inversion was run in a deterministic mode, with signal-to-noise (S/N) ratio volumes being used as weights in the inversion to guide the inversion into not forcing a fit in areas of poor seismic signal. The output volumes were checked at the wells and inverted AI and  $V_p/V_s$  showed excellent agreement with the measured logs (correlations between 0.74-0.95). However the inverted density was slightly noisier, as expected, since density is the hardest to invert from surface seismic, but the inversion was still able to capture the main density changes.

With these inverted elastic attributes, a rock physics inversion was performed to transform these attributes into porosity and mineral volumes. The approach follows the idea of using theoretical and empirical rock physics relationships as a guide for interpreting seismic-derived properties as demonstrated by Johnson et al. (2012) and Mutual et al. (2020).

As mentioned, the Baldonnell Formation is a carbonate reservoir with mixed mineralogy. Core data and regional studies (Mossop and Shetsen, 1994) indicate it is predominantly a dolomitized limestone with minor clastic content (siltstone/shale). A three-mineral model was chosen: clay, calcite, and dolomite. Clay here represents the insoluble depositional residue (siltstone or shale content, generally with clay minerals) that lowers the matrix stiffness, while calcite and dolomite represent the carbonate matrix (calcite for un-dolomitized limestone fraction, dolomite for areas of dolomitization). As dolomite has a higher stiffness (approximate bulk modulus of 95 GPa, and shear modulus of 45 GPa) than calcite (bulk ~70 GPa, shear 30 GPa), so the mineral composition strongly influences elastic velocities.

The rock physics model utilized is based on the work done by Westang et al. in 2009. This model treats the mineral mixture's bulk and shear moduli as an unknown that the inversion can adjust within the Voigt-Reuss-Hill bounds, effectively allowing calibration to local rock stiffnesses. The pore fluid in the Baldonnell is saline water under original in-situ conditions. Since the seismic data available is CO<sub>2</sub> pre-injection (baseline), we assumed 100% brine saturation in the inversion; however, the presence of small amounts of original gas (if any) could be accounted for with Gassmann fluid substitution but was not part of the scope of this study.

Once the calibrated rock physics model for the Baldonnell was completed, the elastic volumes (AI,  $V_p/V_s$ , and to a lesser extent density) were inverted to obtain 3D volumes of porosity, clay volume, and dolomite (with calcite being the remainder to sum to 100%). This is effectively a nonlinear inversion problem as we seek estimates of the porosity and mineral fractions  $V_{clay}$ ,  $V_{dolomite}$  and  $V_{calcite}$  at each point such that the computed AI,  $V_p/V_s$  from the rock physics model match the inverted seismic values. The solution was constrained within reasonable bounds: porosity was allowed to vary between 0 and 30% (in line with the Baldonnell's known range), clay volume between 0 and 0.3 (we assume a maximum of 30% clay in this carbonate, but likely less in most cases), and the dolomite vs calcite mix from 0 to 1 (100% calcite to 100% dolomite). The inversion was carried out by a regression approach at well locations first for calibration and then applied to the whole volume. At the well, petrophysical log-derived porosity and mineralogy (from core/mineral logs or interpreted lithology logs) was used to fine tune the model. After calibration, we applied the inversion across the 3D volume. This essentially entailed computing, at each seismic sample, the combination of porosity,  $V_{clay}$ ,  $V_{dolomite}$  that gives the best match to the seismic-derived AI and  $V_p/V_s$ . While density, being less reliable, was used as a secondary check. In practice, AI and  $V_p/V_s$  primarily constrain the solution as AI is strongly controlled by porosity and mineral bulk modulus, while  $V_p/V_s$  is sensitive to lithology – carbonates vs clastics – and thus helps determine clay content. The result of the rock physics inversion is a 3D porosity volume for the Baldonnell, plus volumes for clay, calcite, and dolomite fractions.

## Results

The deterministic AVO inversion produced volumes of AI,  $V_p/V_s$ , and density for the entire window of interest including the Baldonnell Formation. The Baldonnell Formation appears as a distinct acoustic impedance with mid to low values between higher-impedance contrast units above and below. The results show an excellent agreement with the elastic properties of the well logs throughout the entire window but especially within the Baldonnell thereby being able to discriminate mid AI values within a low AI layer above and a higher

AI layer below (Charlie Lake). Overall, these elastic inversion results matched geological expectations and provided essential inputs to subsequent rock physics inversion and interpretation.

The rock physics inversion, translating elastic attributes into porosity and mineral volumes, resulted in a detailed 3D porosity volume for the Baldonnell Formation, a principal outcome of this study. Porosity ranges between 5% up to approximately 20%, with the highest porosities localized in identifiable trends are shown in Figure 2. Vertically, porosity is predominantly concentrated within the upper section of the formation, with significantly reduced porosity (<5%) towards the lower section. This vertical porosity gradation aligns with regional geological expectations with quantified confirmation from the inversion results. Laterally, the inversion highlights distinct variability likely associated with enhanced dolomitization. Outside this corridor, porosities predominantly range between 5–10%.

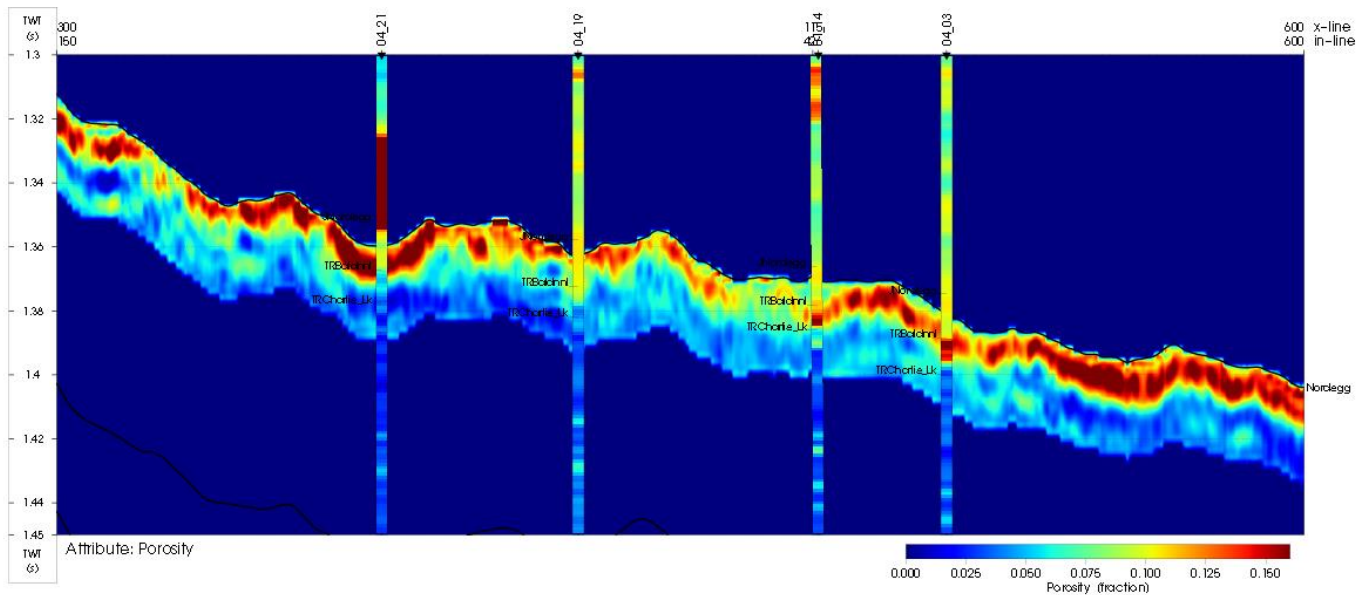


**Figure 2. Total porosity volume across an arbitrary line going through 4 key wells. Most of the well porosity logs are in agreement with the inversion results showing higher porosity values except for the first well from the left that had some logging issues as seen in the mismatch to the other logs above the Nordegg Formation.**

Porosity maps generated through seismic-driven inversion significantly outperform maps relying solely on well log data interpolation as shown in Figure 3. Maps derived exclusively from well data produce broadly uniform porosity distributions, generally lacking spatial detail due to sparse sampling. Conversely, seismic inversion-based maps clearly identify detailed heterogeneities, including high-porosity zones surrounded by lower porosity areas. The inversion-based porosity map precisely locates a high-porosity trend (on the south edge of the 3D) and a potential secondary high-porosity pocket southeast of the existing injector well—critical information for guiding further injection or monitoring well placements.

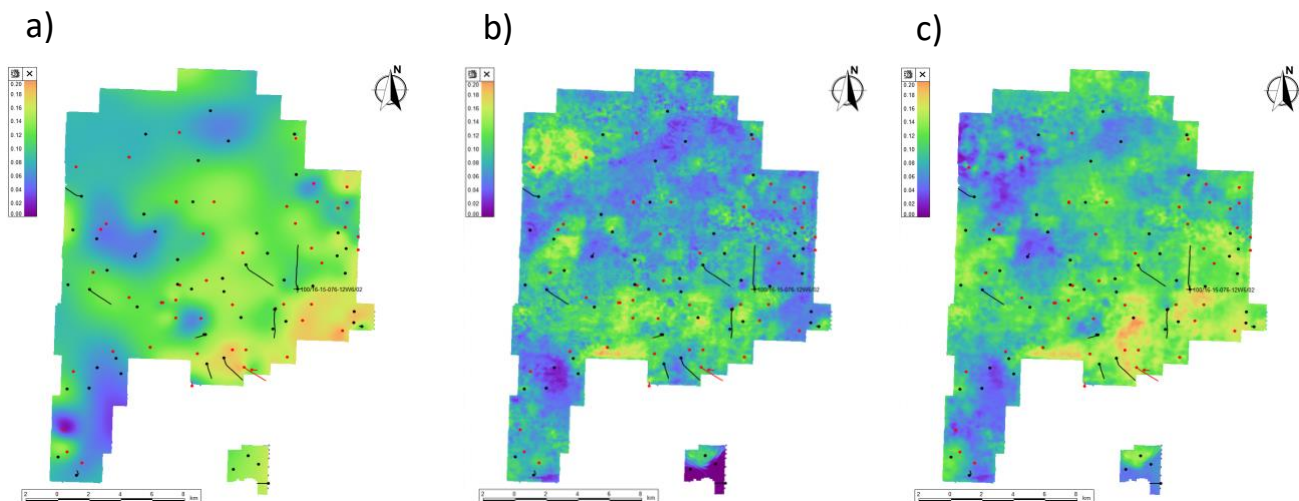




**Figure 3. Comparison of Baldonnell porosity mapping approaches: (a) map derived from well log interpolation (without seismic inversion), and (b) map derived from seismic AVO inversion integrated with rock physics. (c) map derived from integrated geomodel. Warm colors indicate higher porosity. The seismic inversion provides much higher spatial resolution and reveals that is not captured in the well-only map.**

Integration of inversion results into the reservoir model significantly improved the accuracy of reservoir characterization and CO<sub>2</sub> injection planning. Porosity maps derived from seismic inversion, combined with geostatistical methods for porosity interpolation, substantially enhanced the geomodel's predictive power. The integrated geomodel (figure 3c) incorporates porosity logs upscaled into layers with 1-meter thickness, using seismic inversion maps as secondary trends. Upscaled logs predominantly drive porosity distribution, with seismic trends influencing lateral interpolation. Comparisons between the original porosity model and the integrated geomodel illustrate marked improvements, notably in the precision of lateral porosity distribution around the 16-15 CO<sub>2</sub> injector well in the southeast corner of the 3D.

A horizontal CO<sub>2</sub> injector well drilled subsequent to the inversion validated the predicted porosity distributions, particularly confirming the absence of significant porosity in the lower Baldonnell, which the inversion accurately predicted (Figure 4). Injection operations commenced at approximately 40 tonnes of CO<sub>2</sub> per day, with plans to scale up to roughly 500 tonnes per day. Porosity-based volumetric assessments support this operational scale-up, indicating that the reservoir's effective pore volume can accommodate significant CO<sub>2</sub> volumes safely over extended periods.

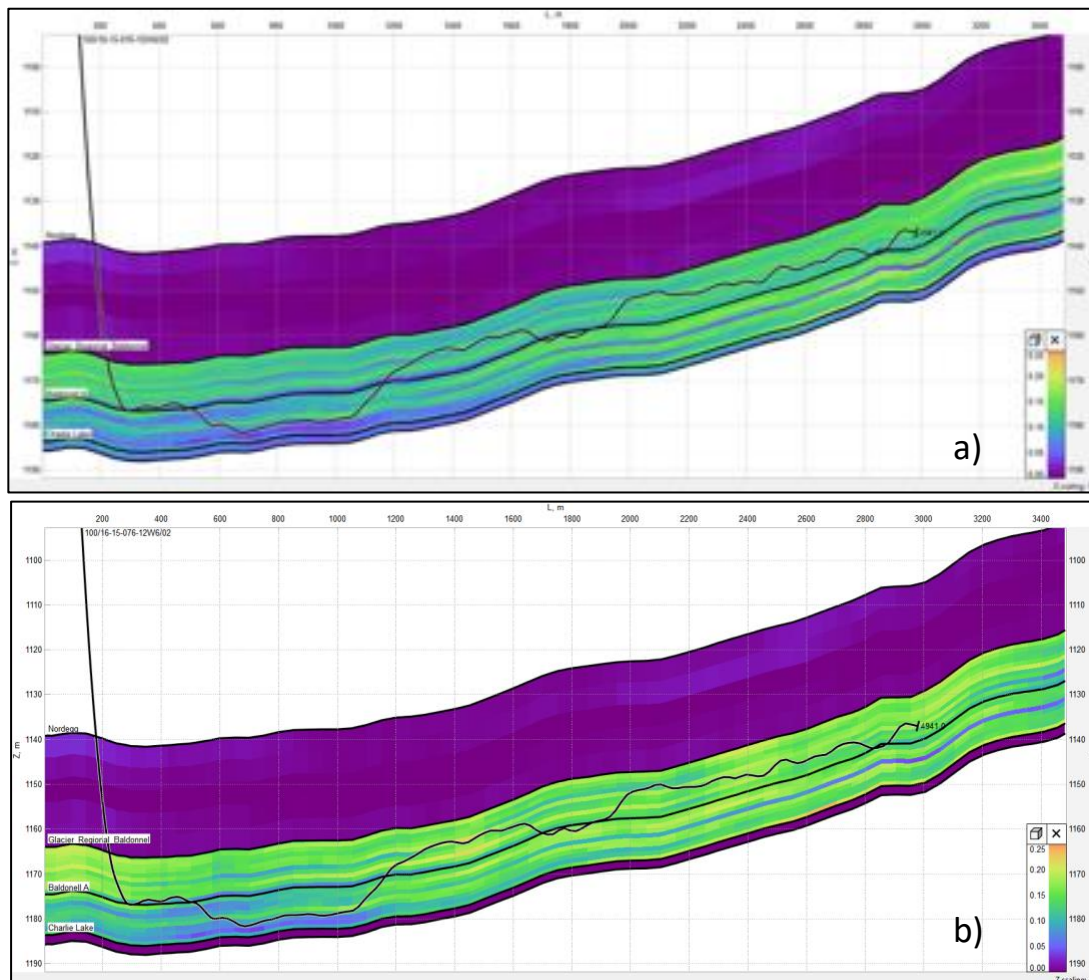


**Figure 4. CO<sub>2</sub> injector section view with porosity model before and after incorporation of inversion results, (a) Injector section with original porosity model, (b) injector section with integrated porosity model.**

## Conclusion

The Baldonnell Formation characterization via deterministic seismic inversion and rock physics modeling provided substantial improvements in understanding reservoir heterogeneity, significantly influencing CO<sub>2</sub> injection planning and operational efficiency.

The inversion-derived porosity and mineral fraction volumes were instrumental in refining reservoir simulations and monitoring strategies, effectively reducing operational risks. This study stands as a benchmark for future CCUS projects, demonstrating the practical application of advanced seismic techniques for detailed and accurate reservoir characterization, ultimately ensuring safe, effective, and optimized CO<sub>2</sub> sequestration. Future studies should incorporate additional well data to refine inversion parameters further, enhance model accuracy, and support long-term monitoring and operational adjustments.

## Acknowledgments

We would like to acknowledge Advantage Energy and Entropy Inc. for the collaboration and permission to show this study. We would also like to thank WesternGeco for data show rights.

## References

- Aki, K., and Richards, P. G., 1980. *Quantitative Seismology: Theory and Methods*. W. H. Freeman and Co.
- Bachu, S., 2015. "Review of CO<sub>2</sub> Storage Efficiency in Deep Saline Aquifers," *International Journal of Greenhouse Gas Control*, 40, 188–202.
- Gassmann, F., 1951. "Über die Elastizität poröser Medien," *Vierteljahrsschrift der Naturforschenden Gesellschaft in Zürich*, 96, 1–23. (English translation: "On the elasticity of porous media.")
- Gordon, A., Goodway, B., Mutual, E., Cova, R., Leaney, S., Pardasie, W., Ng, M., 2023. "Characterizing Multiple Formations for Gas Production and CO<sub>2</sub> Sequestration," 2023, SPE/AAPG/SEG Unconventional Resources Technology Conference. doi: <https://doi.org/10.15530/urtec-2023-3866741>
- Hashin, Z., and Shtrikman, S., 1963. "A Variational Approach to the Theory of the Elastic Behaviour of Polycrystals," *Journal of the Mechanics and Physics of Solids*, 11(2), 127–140.
- Hill, R., 1952. "The Elastic Behaviour of a Crystalline Aggregate," *Proceedings of the Physical Society. Section A*, 65(5), 349–354. (Introduces Voigt–Reuss–Hill averages.)
- IPCC, 2005. *IPCC Special Report on Carbon Dioxide Capture and Storage*. Prepared by Working Group III of the IPCC (Metz, B., et al., Eds.). Cambridge University Press, 442 pp.
- Johnson, J., Holmstrom, L., Diocee, S., Tilson, R., and Johnston, S., 2012. "Rock Physics Inversion: A Montney Case Study," *GeoConvention 2012: Vision*, Expanded Abstracts.
- Mossop, G. D., and Shetsen, I. (compilers), 1994. *Geological Atlas of the Western Canada Sedimentary Basin*. Canadian Society of Petroleum Geologists & Alberta Research Council, Calgary, Chapter 16: Triassic Strata.
- Mutual, E., Mills, A., Cholach, P., Cho, D., and Boskovic, D., 2020. "Beyond Seismic Stack: Rock Physics Inversion for Horizontal Well Placement in Southern Alberta," *SEG Technical Program Expanded Abstracts*, 1206–1209.
- Shuey, R. T., 1985. "A Simplification of the Zoeppritz Equations," *Geophysics*, 50(4), 609–614.
- Westang, K., Hansen, H., and Rasmussen, K., 2009. "ISIS Rock Physics – A New Petro-Elastic Model for Optimal Rock Physics Inversion with Examples from the Nini Field," *Sound of Geology Workshop 2009*, Expanded Abstracts.